Check for updates

Experimental and Numerical Investigation of Plain and Gouged Dents in Steel Pipes Subjected to Pressure and Moment Loading

J. Błachut

I. B. Iflefel

Mechanical Engineering,
The University of Liverpool,
Liverpool L69 3GH, United Kingdom

Six laboratory scale, mild steel pipes with the outside diameter-to-wall-thickness ratio, $D_o/t \cong 40$, were dented to about 15–20% of outside diameter D_o, by a hemispherical indenter with its diameter to pipe's outside diameter ratio, $2a/D_o \cong 0.41$. Three pipes had surface gouges running axially in them, and the remaining three were gouge free. Five of them were then collapsed by a bending moment followed by pressure burst tests. Experimental test data has been used to benchmark the finite element results, details of which are given in this paper. Good agreement between experimental and numerical results was obtained in the modeling of denting, but not so well in the modeling of bending—indicating the need for further work in order to address the discrepancies.
[DOI: 10.1115/1.2891913]

1 Introduction

Typical sources of damage to buried pipelines include earth moving, excavation equipment, or falling objects. The resulting damage can affect the pressure carrying capacity and/or operating life of the pipeline and hence it is important to have guidelines/procedures for the damage assessment. Plain dents and dents with gouges are usually considered as possible causes of pipes' failure, and some aspects of their structural behavior are briefly discussed next.

The behavior of plain dents has been studied extensively in recent years and it appears that plain dents of up to 24% of the diameter may not significantly affect bursting pressure—Ref. [1]. Other aspects of having dents in pipes include change of length, width and shape of the dent, and contact issues between indenter and the pipe's surface and between the pipe and its support. These topics have been studied numerically and the results can be found in Ref. [2]. Reference [3] suggests that gouges placed at two regions of high strains, i.e., at the axial extremities of the initial dent, could affect burst pressure. Mostly experimental work, conducted in Ref. [4], emphasized the influence of soil support, pipe pressure level, magnitude, and orientation of outside force, on damage behavior. Reference [5] has introduced several equations for assessment of gouges in plain pipelines. It transpires that influence of gouges on burst pressure is dependent on their depth, length, and direction. A recent review of the existing experimental and numerical data on dented pipelines can be found in Ref. [6]. A need for "usable guidelines" to be developed in order to assist pipeline operators in their assessments of damaged pipes is made in this reference. Subsequently, a project sponsored by 15 oil and gas companies has produced the pipeline defect assessment manual—see Ref. [7]. The manual lists the best practice for assessing dented pipelines with defects. It also contains guidance for dealing with plain dents, kinked dents, smooth dents on welds, smooth dents containing gouges, and smooth dents containing other types of defects. All of the above references consider internally pressurized pipes. Structural behavior of dented pipes subjected to external pressure has also been studied in the past. For example, results of one such study are reported in Ref. [8], where 37 tests on dented cylinders subjected to hydrostatic pressure were carried out. Collapse pressures were found to be relatively insensitive to detailed geometry of dents.

Reference [9] indicates that the open literature contains data on about 420 experiments with various shapes of indenters applied to pressurized pipes, which had the (D/t) ratios between 18 and 108. The largest number of experiments was carried on pipes with the (D/t) ratio of about 50. It is worth noting that experimental treatment of dented pipes in which dents contain gouges is less frequent. Two such sets of experiments are mentioned next. The results of 24 tests on laboratory scale aluminum pipes are reported in Ref. [10]. Depth of dents and dimensions of gouges are given, for completeness, in Table 1, rows 1–24. All gouges were introduced to the external surface and all of them were axial. The next set is given in Reference [11]. Details of experimental and linear elastic finite element investigations into stress levels in mild steel pipes containing dents with external longitudinal gouges are provided. Authors report results from burst tests on dented pipes and compare the data with existing prediction procedures at that time. Dimensions of surface defects treated experimentally in Ref. [11] are also given in Table 1, rows 25–40. A common denominator of laboratory scale tests described in Refs. [10,11] is hemispherical shape of the indenter. The range of studied geometries in Refs. [9–11] influenced the choice of the (D/t) ratio adopted in the current paper, i.e., $D/t \approx 40$.

Dented pipes can be subjected to bending moment as a result of earth movement or due to the underwater currents. This has been addressed by a study of two types of bending moment, i.e., closing bending moment (CBM) and opening bending moment (OBM)—as illustrated in Fig. 1. The results of such, entirely numerical investigation, can be found in Ref. [12].

It is felt that tests on a carefully selected series of dented and gouged dents in a pipeline, together with backup finite element (FE) numerical analysis, would provide data that could be used to validate or modify the new and/or existing assessment procedures that are currently being developed by the pipeline operators. With this in mind, the current paper details experimental work on damaged, laboratory scale, mild steel pipes collapsed by bending moment. Details about the corresponding FE calculations are also given.

Contributed by the Pressure Vessel and Piping Division of ASME for publishing in the JOURNAL OF PRESSURE VESSEL TECHNOLOGY. Manuscript received August 1, 2006; final manuscript received August 22, 2007; published online March 31, 2008. Review conducted by Maher Y. A. Younan. Paper presented at the 2006 ASME Pressure Vessels and Piping Conference (PVP2006), Vancouver, British Columbia, Canada, July 23–27, 2006.

 Copyright © 2008 by ASME

Downloaded from http://asmedigitalcollection.asme.org/pressurevesseltech/article-pdf/130/2/021203/5534545/021203_1.pdf by guest on 05 November 2024

Table 1 Geometry of aluminium Models 1–24 is taken from Ref. [10]. Data for the remaining mild steel models are taken from Ref. [11]. All gouges were axial. All models were dented under zero internal pressure, except Entries 12 and 13. Entries 17–24 had axial gouges at the midlength but they were offset to a side.

							Gouge		
No.	D_o (mm)	t (mm)	$2a$ (mm)	L (mm)	δ/D_o (%)	D_o/t	$2c/D_o$ (%)	e/t (%)	σ_{yp} (MPa)
1	100	1.848	50.8	338	4.9	54.1	25.4	14.1	163.0
2	100	1.848	50.8	338	4.3	54.1	25.4	31.7	163.0
3	100	1.848	50.8	338	6.4	54.1	25.4	47.0	163.0
4	100	1.848	50.8	338	9.7	54.1	25.4	0.0	163.0
5	100	1.848	50.8	338	10.8	54.1	25.4	15.2	163.0
6	100	1.848	50.8	338	10.2	54.1	25.4	30.3	163.0
7	100	1.848	50.8	338	10.6	54.1	25.4	45.4	163.0
8	100	1.848	50.8	338	15.8	54.1	25.4	0.0	163.0
9	100	1.848	50.8	338	15.1	54.1	25.4	15.3	163.0
10	100	1.848	50.8	338	15.2	54.1	25.4	29.7	163.0
11	100	1.848	50.8	338	15.3	54.1	25.4	45.5	163.0
12	100	1.848	50.8	338	7.2	54.1	25.4	44.3	163.0
13	100	1.848	50.8	338	9.1	54.1	25.4	48.6	163.0
14	100	1.848	50.8	338	13.2	54.1	50.8	44.4	163.0
15	100	1.848	50.8	338	14.9	54.1	50.8	45.4	163.0
16	100	1.848	50.8	338	12.1	54.1	280.0	31.8	163.0
17	100	1.848	50.8	338	11.7	54.1	25.4	45.0	163.0
18	100	1.848	50.8	338	11.9	54.1	25.4	55.0	163.0
19	100	1.848	50.8	338	11.8	54.1	25.4	45.1	163.0
20	100	1.848	50.8	338	13.0	54.1	25.4	56.2	163.0
21	100	1.848	50.8	338	12.0	54.1	25.4	46.6	163.0
22	100	1.848	50.8	338	12.1	54.1	25.4	43.9	163.0
23	100	1.848	50.8	338	12.3	54.1	25.4	48.2	163.0
24	100	1.848	50.8	338	11.9	54.1	25.4	46.0	163.0
25	160.20	2.20	63.5	900	8.5	72.8	47.8	21.8	294.0
26	161.63	1.63	63.5	900	10.0	99.0	47.8	44.3	294.0
27	161.60	1.60	63.5	900	6.0	101.	47.8	45.0	294.0
28	162.35	2.35	63.5	900	6.0	69.1	47.8	40.8	294.0
29	161.70	1.70	63.5	900	6.0	95.1	47.8	28.2	294.0
30	162.31	2.31	63.5	900	10.0	70.3	47.8	10.4	294.0
31	162.10	2.10	63.5	900	6.0	77.2	47.8	11.4	294.0
32	161.60	1.60	63.5	900	2.0	101.	47.8	45.0	294.0
33	161.50	1.50	63.5	900	2.0	108.	47.8	32.0	294.0
34	162.20	2.20	63.5	900	2.0	73.7	47.8	10.9	294.0
35	161.66	1.66	63.5	900	4.0	97.4	47.8	28.9	294.0
36	161.86	1.86	63.5	900	4.0	87.0	47.8	12.9	294.0
36	162.20	2.20	63.5	900	4.0	73.7	47.8	21.8	294.0
37	162.00	2.00	63.5	900	4.0	81.0	47.8	36.0	294.0
38	161.85	1.85	63.5	900	10.0	87.5	47.8	25.9	294.0
39	162.10	2.10	63.5	900	8.0	77.2	47.8	11.4	294.0
40	161.70	1.70	63.5	900	8.0	95.1	47.8	28.2	294.0

2 Model Preparation

All models were made by machining 5.7 mm thick, mild steel pipe from inside and outside to secure the outside diameter-to-wall thickness ratio, $D_o/t \cong 40$. The initial length of the pipe was about 610 mm and it was cut into three pieces, P1, P2, and P3—as shown in Fig. 2(*a*). This was done in order to minimize the pipe's vibrations during CNC machining. Length of the middle portion was nominally, $3D_o$, with the other two parts having equal length of $1.5D_o$. Nominal wall thickness of all three parts was the same, $t=2.1$ mm. All three parts were subsequently welded and an additional extension, 250 mm long and 6.75 mm thick, added at both ends. The above arrangements are depicted in Figs. 2(*a*) and 2(*b*). Six such pipe models were prepared and they are designated here as SP1, SP2, …, SP6.

The first three specimens were machined without surface defects whereas the remaining three were manufactured with surface

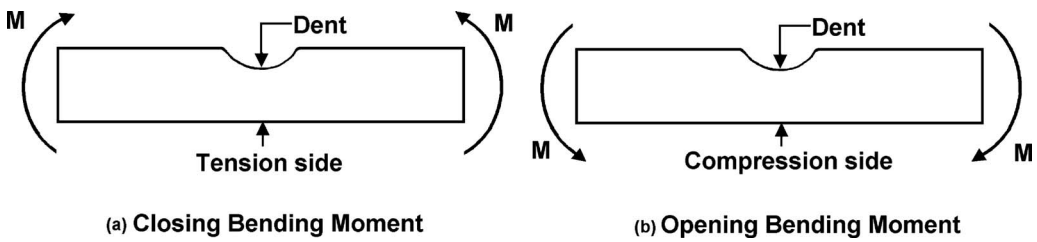

Fig. 1 Sketch illustrating loading of a dented pipe by opening and closing bending moment

Downloaded from http://asmedigitalcollection.asme.org/pressurevesseltech/article-pdf/130/2/021203/5534545/021203_1.pdf by guest on 05 November 2024

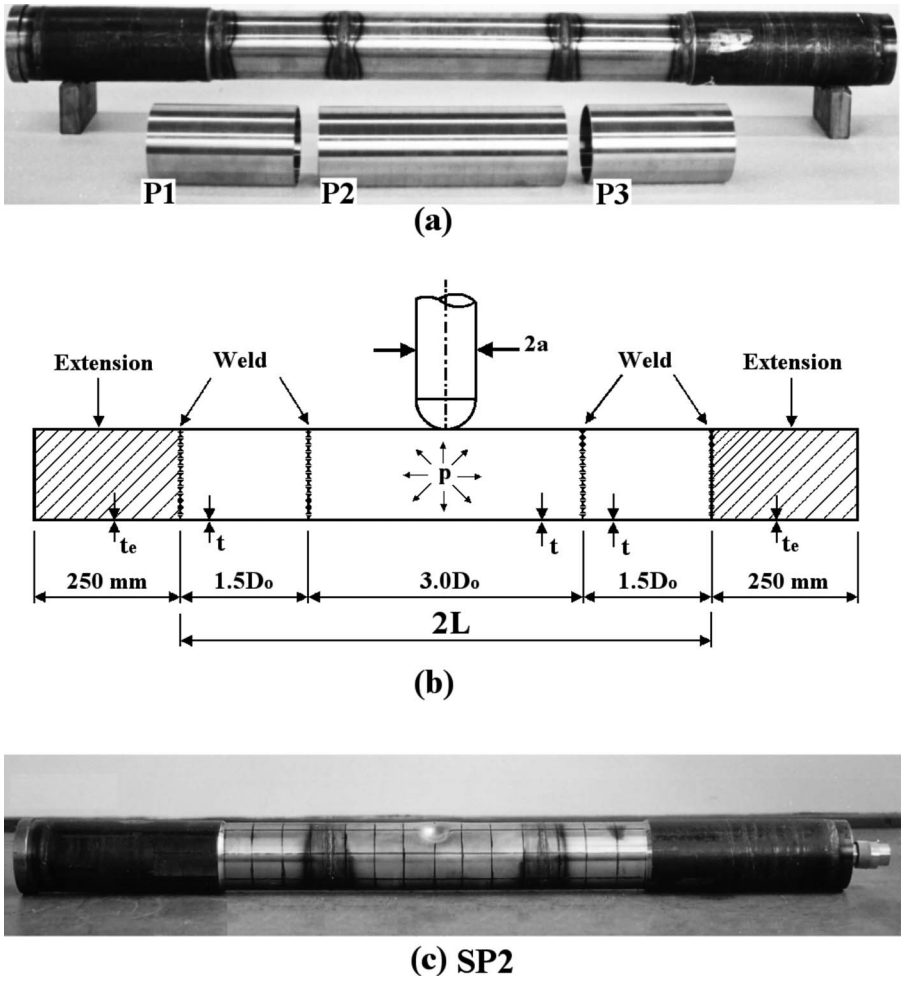

Fig. 2 View of Parts P1, P2, and P3 after CNC machining and after welding. Two thicker extensions at both ends are also shown (*a*). Sketch depicting dimensions of various parts together with a vertical indenter (*b*). View of a plain pipe after denting with internal pressure released to zero (*c*).

defects running axially. A single axial gouge was introduced at the center of anticipated dent in the fourth model. Two gouges, of the same dimensions, were introduced on peripheries of anticipated dent in the fifth pipe. Electrical discharge machine was used to create these defects. The sixth pipe had a larger defect introduced at the center of anticipated dent. The latter was introduced by standard machining.

Defects introduced by the EDM technique had the depth-to-wall-thickness ratio, $e/t \cong 0.47$, the length-to-outside-diameter ratio, $2c/D_o \cong 0.25$, and the width-to-wall-thickness ratio, $2w/t \cong 0.50$. The machined gouge had these ratios given by $e/t \cong 0.23$, $2c/D_o \cong 0.81$, and $2w/t \cong 1.20$. All gouges were introduced to part P2 prior to welding and prior to denting, i.e., they were introduced into the "near perfect" pipe's geometry. Figure 3 illustrates these arrangements and a view of an axial, machined notch is shown in Fig. 4(*b*). Prior to testing geometry of all pipes was measured. Wall thickness was measured at 10 mm intervals in axial direction and at 15 mm in hoop direction. Pipes were also checked for straightness and for any ovalization. Average values of obtained results are provided in Table 2.

2.1 Pipe Support, Indenter, and Material Properties. During denting, each pipe was supported by a wooden, saddle type support of length $6D_o$. Its hoop span was 120 deg (see Refs. [2,9] for further details). Material properties of steel pipes have been found from uniaxial tests of coupons cut out from a pipe in longitudinal direction. These were subsequently machined flat with a nominal thickness of 2.37 mm and 20.0 mm width. A typical stress-strain curve, obtained for flat coupons, is shown in Fig. 5. Average values of obtained results are given in Table 3. Stiffness of wooden support has also been evaluated experimentally by testing $25.8 \times 26.1 \times 25$ mm^3 block of wood in compression. Compressive force versus displacement is depicted in Fig. 6(*a*). This curve was subsequently used for the FE modeling of pipe support (see later). A solid, hemispherical indenter made from mild steel was used throughout. Its diameter, $2a$, was 34.7 mm and Figs. 2(*b*) and 4(b1) show the arrangements, which were used.

2.2 Denting Process. It is seen from Table 2 that all pipes were dented. Model SP1 was dented with no internal pressure, while the other pipes were pressurized prior to denting. The pressure level was maintained constant during denting. Denting has been carried out by pressing a hemispherical indenter to a prescribed depth given in column 4 of Table 4. Nongouged pipes, i.e., SP2 and SP3, were pressurized to design pressure, $p=11.2$ MPa, while all gouged pipes, i.e., SP4, SP5, and SP6 were pressurized to 50% of that value, i.e., $p=5.6$ MPa. Speed of denting was 0.1 mm/min. After reaching the prescribed depth of the dent, the indenter has been removed and internal pressure was released to zero. This caused some elastic spring back of the dent, and column 6 in Table 4 contains the final depth recorded for each pipe measured at zero pressure, $(\delta/D_o)_R$. Figure 2(*c*) depicts a dent

Downloaded from http://asmedigitalcollection.asme.org/pressurevesseltech/article-pdf/130/2/021203/5534545/021203_1.pdf by guest on 05 November 2024

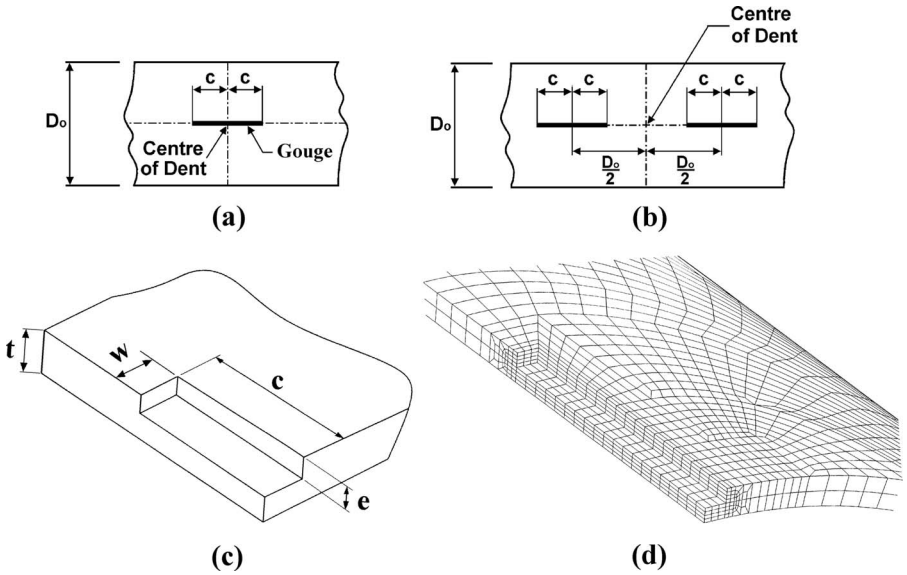

Fig. 3 Position of axial gouges of length 2*c* with respect to the midspan of pipe (*a*) and (*b*). Also, notation for the FE modeling (*c*). Typical FE meshing of a gouge (*d*).

after removal of the indenter, followed by release of pressure to zero in a nongouged pipe. Figure 4, on the other hand, shows a closer view of part P2 for various models and at various stages of the experiment. Profiles of dents have been measured after completion of denting and at zero pressure. Typical plot of denting force versus depth of indentation is seen in Fig. 7(*a*) for the pipe SP5 while axial profile of the resulting dent is shown in Fig. 7(*b*) (half of its actual axial length). Full comparison of experimental results with the FE predictions is given later.

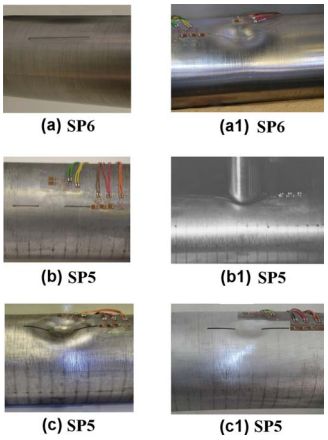

Fig. 4 Photographs of gouged Pipes SP5 and SP6 at different stages of experimentation

3 Bending of Pipes

Five pipes were subjected to bending after they have undergone denting. Arrangements for four-point bending are sketched in Fig. 8(*a*) for the case of OBM. It is seen from Fig. 8(*a*) that in order to avoid a local damage/buckling of the wall, two slightly thicker pipe ends were welded to each pipe. Rotation of a pipe has been obtained from two light probes, TR1 and TR2, attached to the pipe, as shown in Fig. 8. A photograph showing a bent pipe in the bending rig is depicted in Fig. 8(*b*), and a typical plot of bending moment versus pipe rotation is displayed in Fig. 9(*a*)—for the Shell SP3. Similar response has been obtained for the Pipe SP5, shown in Fig. 9(*b*). Prior to bending, all pipes were pressurized to $p_{\text{bending}}=5.6$ MPa. This magnitude corresponds to 50% of a design pressure for nongouged, perfect pipe. The level of pressure was kept constant during bending. This was achieved by having a pressure compensator attached (see Ref. [9]). Loading was controlled by vertical displacement. Its speed rate was 0.1 mm/min. Loading was stopped once buckles developed in the pipe. For CBM, bulges appeared on both sides of the dent—as shown in Fig. 10(*a*). In the case of the OBM, buckles/bulges appeared on the opposite side of the dent near "P1-P2" and "P2-P3" junctions—see Fig. 10(*b*). The maximum recorded forces, for Shells SP2, …, SP6 were in the

Table 2 Geometry of six mild steel pipes. Also, values of internal pressure during denting, indication whether the pipe was gouged and whether it was subsequently bent. In all cases, the indenter had a hemispherical shape with $2a/D_o=0.41$.

Model	D_o (mm)	t (mm)	L (mm)	p_{denting} (MPa)	Gouged	Bent
SP1	84.20	2.07	505.2	0.0	No	No
SP2	84.10	2.10	504.6	11.2	No	Yes
SP3	84.08	2.08	504.5	11.2	No	Yes
SP4	84.06	2.09	504.4	5.6	Yes	Yes
SP5	84.08	2.08	504.5	5.6	Yes	Yes
SP6	83.97	2.08	503.8	5.6	Yes	Yes

Downloaded from http://asmedigitalcollection.asme.org/pressurevesseltech/article-pdf/130/2/021203/5534545/021203_1.pdf by guest on 05 November 2024

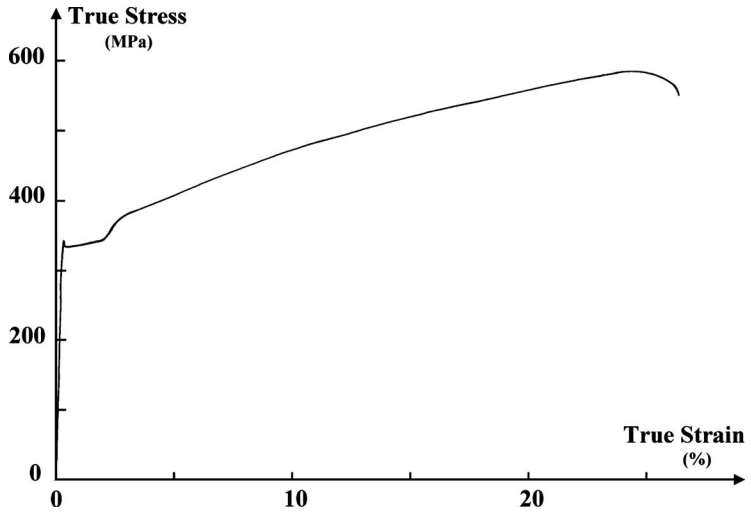

Fig. 5 Typical stress-strain curve of pipe material obtained from uniaxial tensile test of a flat test piece

range of 59.0 and 72.0 kN. These values were converted to maximum bending moments $(BM)_{max}$, and their values are provided in Table 4.

Maximum rotation of pipes, at collapse, was calculated from TR1/TR2 readings and the corresponding results are also given in Table 4. It is seen here that gouged models collapsed at bending moments not more than 15% below corresponding values for nongouged Pipes SP2 and SP3. There is also a small difference in the load carrying capacity between loading by the OBM and by the CBM. The latter loading mode appears to be the most detrimental although this is not a like-for-like comparison due to the existence of different defects.

4 FE Modeling and Analysis

4.1 Modeling of Dents. The FE models were constructed using PATRAN [13] and subsequent stress analysis was conducted using the FE code ABAQUS, Ref. [14]. Due to the symmetry of the problem, a quarter FE model, with the axial length of $3D_o$, was adopted, and Fig. 11(*a*) shows a typical mesh used in computations. Appropriate boundary conditions have been applied along all four edges of pipe's quarter model. These were deduced from the symmetry conditions. The indenter was allowed to move only in vertical direction and the wooden support was fixed at the bottom. Detailed account of boundary conditions used can be found in Ref. [2]. Central area around anticipated dent was modeled using 20-node, reduced integration brick elements, C3D20R. Computations have shown that it was sufficient to use two layers of brick elements through the wall thickness. Two types of the FE models were constructed, i.e., a plain pipe without any surface defect for Models SP1, SP2, and SP3, and plain pipe with axial gouges in Pipes SP4, SP5, and SP6. The analytical rigid surface, used in ABAQUS, was adopted for modeling the indenter. Saddle support of pipes was also modeled as a rigid surface. Saddle support extended the full length of the pipe, and 120 deg in the hoop direction. Both rigid surfaces were available in ABAQUS as "analytical surfaces." The advantage of using the analytical rigid surface option in ABAQUS is associated with smaller computational effort when compared with the use of rigid elements. More details about FE modeling procedure of pipes without defects can be found in Refs. [2,9].

Three FE models were prepared for gouged pipes, i.e., (a) with a single gouge at the center—for SP4, (b) with two gouges at the center—for SP5, and (c) machined gouge at the center—for SP6.

Table 3 Average longitudinal material properties of tested pipes obtained from uniaxial tests on flat coupons

E (GPa)	σ_{yp} (MPa)	ν	σ_{UTS} (MPa)	Applicable to models
210.0	317.0	0.30	460.0	SP1, SP2
205.0	332.0	0.284	459.0	SP3, SP4, SP5, SP6

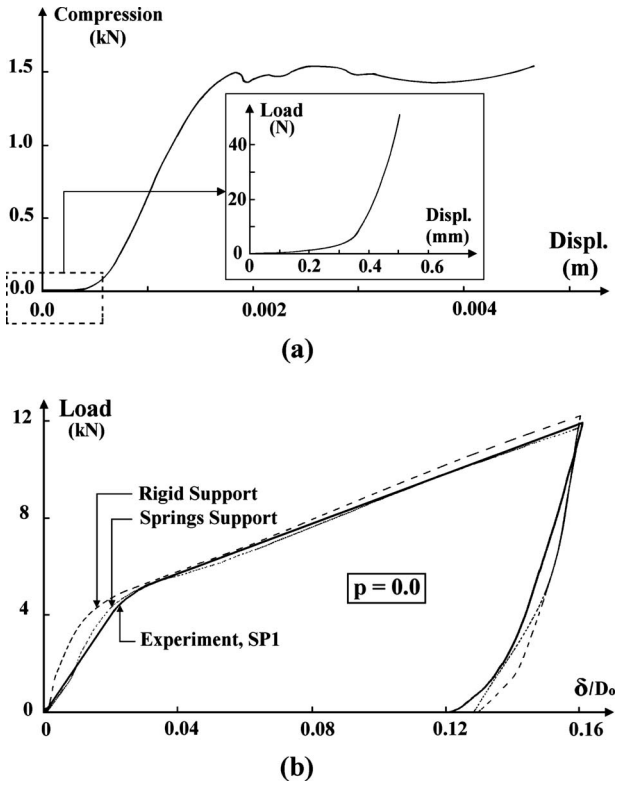

Fig. 6 Load versus deflection for a compressed block of wood used for a saddle support of a steel pipe (*a*). Comparison of experimental denting force versus dent's depth curve with the FE results (*b*). The latter are based on modeling the support as rigid or as a support formed from elastic springs.

Downloaded from http://asmedigitalcollection.asme.org/pressurevesseltech/article-pdf/130/2/021203/5534545/021203_1.pdf by guest on 05 November 2024

Table 4 Comparison of experimental and computed results for denting and bending of plain and gouged pipes. Note: (12.31) ≡corresponds to rigid support of model SP1

	Denting						Bending			
	F_{max} (kN)		$(\delta/D_o)_{max}$ (%)		$(\delta/D_o)_R$ (%)		$(BM)_{max}$ (kN m)		$(Rotation)_{max}$ (rad)	
	Expt.	FE	Expt.	FE	Expt.	FE	Expt.	FE	Expt.	FE
SP1	11.7	12.11(12.31)	16.0	16.0	11.91	12.30	...	...	...	...
SP2	37.0	45.0	23.0	23.0	11.99	13.4	6.15	5.0	0.200	0.220
SP3	39.0	46.0	23.0	23.0	11.77	12.30	6.0	4.96	0.214	0.220
SP4	20.0	22.0	15.0	15.0	9.20	10.70	5.16	4.20	0.216	0.055
SP5	21.5	23.9	16.6	16.6	10.10	11.5	5.79	4.60	0.176	0.206
SP6	21.0	22.4	16.0	16.6	10.20	11.8	5.85	4.90	0.200	0.230

These defects corresponded to experimental models described earlier. All defects, as mentioned previously, were axial and located at the midspan of the pipe. Figures 3(*a*)–3(*c*) show the position and notation used for gouges in pipes.

4.2 Modeling of Gouges. The FE model was constructed first as a flat plate made from several solid sections. Next, the FE mesh was generated for each section, with checks for any duplicate nodes, cracks, etc., being performed. There were two areas where the mesh had to be refined, i.e., at indenter/pipe interface and at the gouge itself.

Vicinity of gouges was modeled with eight brick elements through the thickness and this was reduced to two brick elements further away from the gouge. Once "a flat FE model" was complete, "NMAP" feature in ABAQUS was used to map the plate into a pipe. Advantages of this method include a relative ease of mesh refinement and control of element aspect ratio. These features can be applied before node mapping into pipe's geometry takes place. Figure 3(*d*) illustrates typical meshing around an axial gouge. Table 5 provides data about geometry of gouges in Models SP4, SP5, and SP6.

4.3 Denting and Bending. Prior to bending, pipes were subjected to indentation. There were two contact areas during the analysis, i.e., contact between hemispherical indenter and the pipe and between the pipe and its saddle support. The master-slave algorithm available in ABAQUS was employed here. Denting of each pipe was controlled by master node. Magnitude of its vertical movement was prescribed in advance. The FE analyses included the "NLGEOM" option in order to account for both material and geometry nonlinearity and large deformations. Coefficient of friction between contacting surfaces was assumed as 0.3. Two views of pipe being dented are depicted in Fig. 11. Figure 11(*a*) shows a side view of a pipe and the indenter. Figure 11(*b*) shows a closer view of the pipe being dented. Two layers of brick elements through the wall thickness are clearly visible. After reaching the

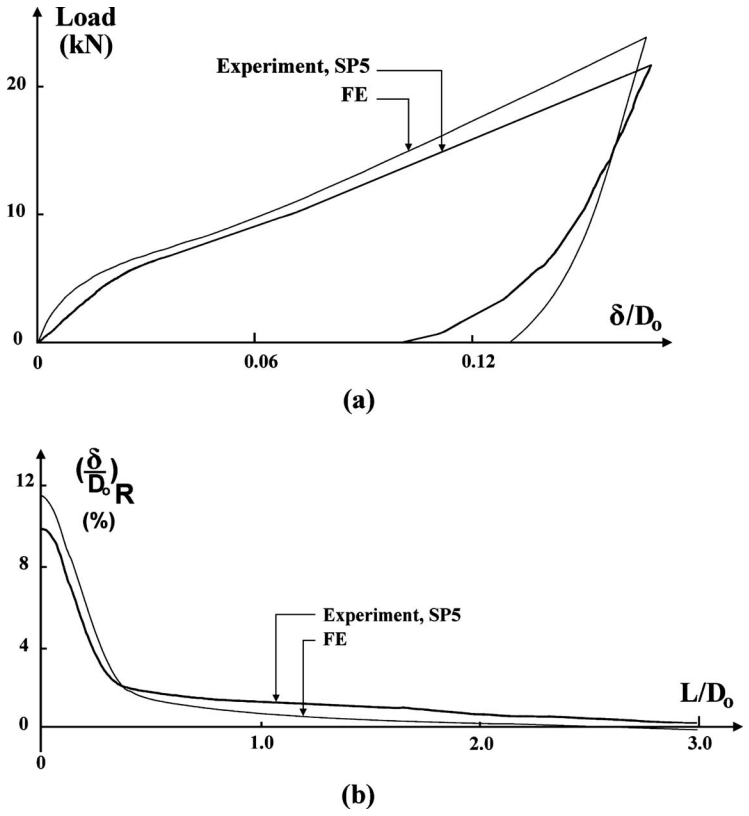

Fig. 7 Comparison of denting force versus depth of the dent with FE results for model SP5 (*a*). Experimental and computed shapes of dented profile along the axial direction (at the end of denting of model SP5) (*b*).

Downloaded from http://asmedigitalcollection.asme.org/pressurevesseltech/article-pdf/130/2/021203/5534545/021203_1.pdf by guest on 05 November 2024

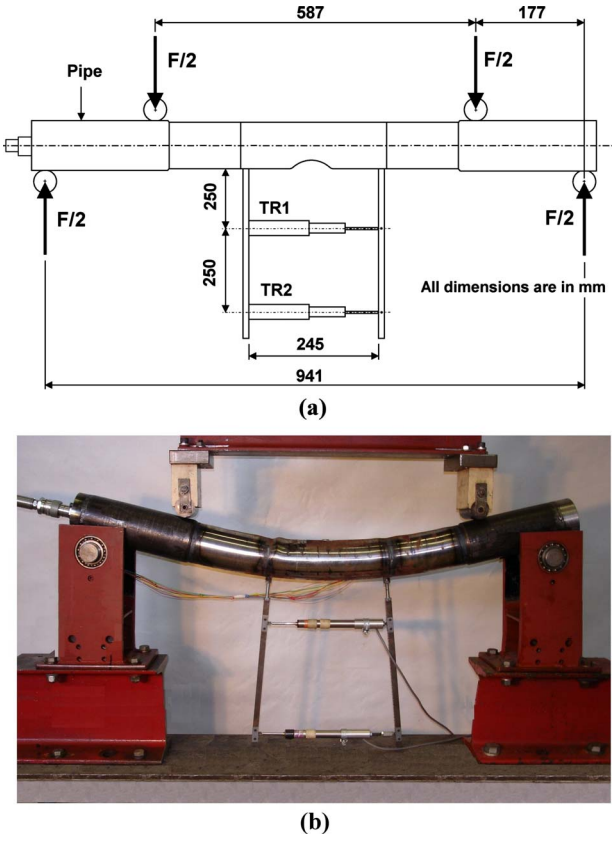

Fig. 8 Arrangements for four-point bending of dented pipe. OBM configuration is shown (*a*). Also, a view of bent pipe in experimental rig (*b*).

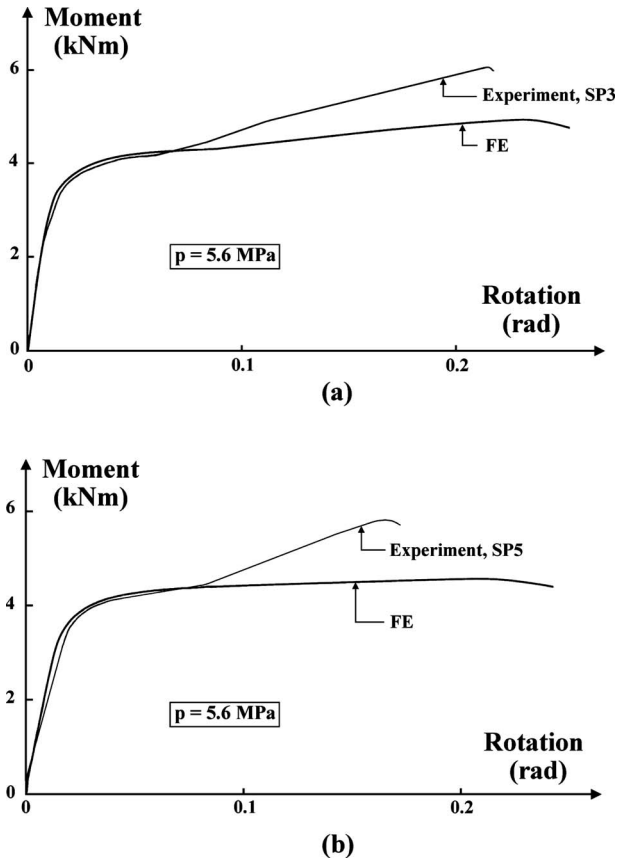

Fig. 9 Comparison of experimental OBM loading versus pipe rotation, with the FE predictions: (*a*) for model SP3 and (*b*) for SP5. Note that welds at Junctions P1/P2 and P2/P3 was not included in the FE analysis.

prescribed depth, the indenter was removed. In the case of pressurized pipes, the pressure was released to zero. In the latter case, there was some spring back of pipe's wall. Figure 2(*c*) depicts the resulting dent in a plain pipe, and Fig. 7(*a*) shows the whole loading and unloading paths for Model SP5. The corresponding experimental curve is also shown on this figure. Axial profile of the dent is plotted, for Model SP5 in Fig. 7(*b*)—where it is seen that the curve follows variation of the dent's depth measured experimentally.

Once the denting procedure was completed, the denting data, such as deformed shape, residual stress, etc., were stored for the second stage of the analysis, i.e., analysis of loading by bending moment. The nodes at the end of the pipe were connected to a master node at the pipe's center. Multipoint constraints technique was then used to impose the end-moment loading (via rotation of the master node). The bending moment analysis started from the last step/increment in denting analysis using "RESTART" option in ABAQUS. This was done to ensure that the residual stresses introduced as a result of the denting process were carried forward into the second phase of the analysis. The restart option contains several actions and they can be summarized as follows: (a) rigid support and the indenter were removed using "MODEL CHANGE" option (with one node being fixed to prevent rigid body motion), (b) pressurize the FE model to the required level, and (c) apply a bending moment via rotation of the master node until bulging occurs (this was done by applying the Riks method). It is worth noting here that application of OBM or CBM remains very simple when the above approach is used.

Typical plots of computed bending moment versus pipe's rotation are shown in Fig. 9. Two types of meshing were tried for the pipe itself. The first was "uniform" mesh but it did not perform well in the contact area. The second mesh used concentric layout of meshing around the dent—see Fig. 3(*d*). This "tuned" meshing performed well and it was adopted for all FE calculations discussed in this paper. Also, checks were performed on the number of elements through the wall thickness. The results have shown that two layers of brick elements were the best choice. The adopted mesh had the elements' aspect ratio not greater than 3:1. Further details about modeling, convergence studies, etc., can be found in Refs. [2,9].

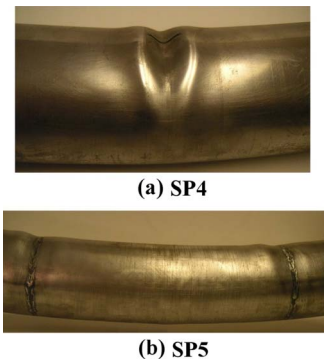

Fig. 10 Photographs depicting bulges in pipes at the maximum, collapsing bending moments for the cases of CBM (*a*) and OBM (*b*).

Downloaded from http://asmedigitalcollection.asme.org/pressurevesseltech/article-pdf/130/2/021203/5534545/021203_1.pdf by guest on 05 November 2024

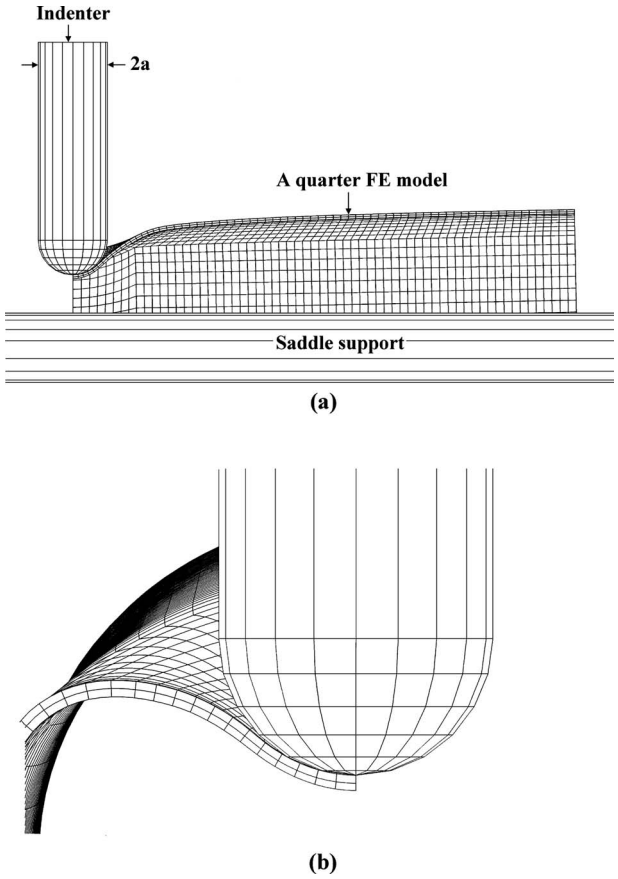

Fig. 11 A section through a pipe subjected to a perpendicular indentation (*a*) (only quarter of pipe is modeled, while the indenter is depicted in its entirety). Also, view down the pipe from the midspan (*b*)

5 Comparison of Experimental and Numerical Results

Comparison of experimental results obtained during denting, being followed by bending, with relevant numerical results is given in Table 4. The ratio of experimentally measured depth of dents after completion of denting and removal of pressure to the same ratio of results obtained numerically varies from 1.03 to 1.16 (Columns 6 and 7 in Table 4). Similar ratio for the magnitude of denting force varies from 1.03 to 1.21 (Columns 2 and 3 in Table 4). It is worth noting here that Models SP2 and SP3 were dented to $0.23D_o$ and largest discrepancies occurred for these models. One possible explanation of these discrepancies could be associated with the use of wrong magnitude of coefficient of friction (value of 0.3 was used throughout). Past calculations have shown that contact pattern between rigid indenter and pipe changes as dent's depth grows. Contact patches have been measured experimentally and they correspond well to the change of patches observed during calculations—see Ref. [9] for further details. It is also seen from Fig. 6 that there is a discrepancy between experiment and numerically simulated slope on the denting force versus dent's depth graph. This discrepancy is larger during the initial phase of loading. This has been investigated a bit further by analyzing stiffness of wooden support. A block of wood, from which the saddle support was manufactured, was tested in order to extract wood's stiffness. Next, the pipe's support was modeled not as rigid but by a set of elastic springs with the stiffness derived from Fig. 6(*a*). Springs were attached to the pipe at all these nodes where previously saddle support was. The obtained response curve is also plotted in Fig. 6(*b*). It is seen that much improved curve, i.e., more closely following the experiment, was obtained. For example, the magnitude of denting force based on rigid support was, for SP1, $F_{max}=12.1$ kN while it was $F_{max}=11.6$ kN for pipe being supported by springs. The latter value compares excellently with the experimental magnitude, $F_{max}=11.7$ kN. The remaining results quoted in Table 4 are provided only for rigid support of the pipe.

The ratio of experimental collapse bending moment to the corresponding FE values varies from 1.20 to 1.23. It is seen from Fig. 9, for example, that the experimental and FE results start to diverge for rotations greater than about 0.07 rad and reaching the above discrepancies at the collapse. The FE results level off while experimental rotations still grow reaching a well defined collapse. Cause of these discrepancies is being investigated.

For the case of the OBM, one possible source of the disparity might be associated with the discontinuity in the vicinity of the girth of welds (between pipe sections P1/P2 and P2/P3). A similar disparity between test data and the FE predictions can be found in Ref. [15] where a different FE software was used, and the running pipe was not welded as in this paper.

6 Closure: Further Work

Some additional studies need to be carried out before some definitive conclusions could be made. To this end, support of the pipe needs to be considered in greater details. At the moment, it is unclear how sensitive collapse bending moments are to the realistic support conditions. Surface gouges considered in the current paper had rectangular shape cross section. Semicircular and V-shaped gouges were studied by others. It is clear that a more comprehensive approach is needed here, as well. Collapse by bending moments, whether open or closing, needs to be extended into postcollapse regime in order to assess severity of this type of failure. Pipes with higher pressures than those considered in this paper need also to be examined for collapse by bending moments in order to obtain a wider working envelope of results. It is worth pointing out that pressure tightness has not been lost in all three dented/gouged pipes for up to the collapse by opening/closing bending moments.

Adopted value of coefficient of friction appears to give reasonable agreement of the FE and experimental results. This might not be true for deeper dents hence further investigations here are needed.

Table 5 Details about pipes subjected to bending. Models SP2 and SP3 had plain dents in them while Models SP4, SP5, and SP6 were gouged.

Model	e/t (%)	$2c/D_o$ (%)	w/t (%)	$p_{bending}$ (MPa)	Bending type
SP2	—	—	—	5.6	OBM
SP3	—	—	—	5.6	OBM
SP4	50	24.98	47.85	5.6	CBM
SP5	50	24.98	48.08[a]	5.6	OBM
SP6	25	80.98	120.2	5.6	OBM

[a]Model SP5 had two axial gauges of the same geometry and placed symmetrically with respect to the midlength.

Downloaded from http://asmedigitalcollection.asme.org/pressurevesseltech/article-pdf/130/2/021203/5534545/021203_1.pdf by guest on 05 November 2024

Finally, the FE underprediction of the magnitude of collapse bending moments has been reconfirmed experimentally and there are no obvious reasons for the disparity. Hence, additional studies appear well justified here.

Nomenclature

$2a$ = indenter's diameter
c = half length of axial gouge (Fig. 3(c))
e = depth of axial gouge running longitudinally (Fig. 3(c))
gouge = machined or spark eroded longitudinal notch (Fig. 3)
p = internal pressure
p_{bending} = magnitude of pressure during bending
p_{denting} = magnitude of pressure during denting
t = pipe wall thickness
w = half of gouge width (Fig. 3(c))
$(\text{BM})_{\text{max}}$ = maximum value of bending moment
D_o = outside diameter of pipe
E = Young's modulus
F_{max} = maximum value of denting force
$2L$ = length of pipe ($2L=6D_o$, see Fig. 1(b))
CNC = computer numerical machining
EDM = electrical discharge machine
TR1, TR2 = displacement transducers (see Fig. 8(a))
δ = radial depth of dent
ν = Poisson's ratio
σ_{yp} = yield point of pipe material
σ_{UTS} = ultimate tensile strength
$(\delta/D_o)_R$ = residual/permanent depth of dent at zero pressure and after elastic spring back

References

[1] Hopkins, P., Jones, D. G., and Clyne, A. J., 1989, "The Significance of Dents and Defects in Transmission Pipelines," Proc. Inst. Mech. Eng. Part E: J. Process Eng., **203**, pp. 137–145.

[2] Błachut, J., and Iflefel,I. B., 2005, "Analysis of Steel Pipelines With Plain and Gouged Dents," *Proceedings of the Tenth International Conference on Civil, Structural and Environmental Engineering Computing*, Rome, Italy, B. H. V. Topping, ed., Civil-Comp, pp. 1–24.

[3] Lancaster, E. R., and Palmer, S. C., 1996, "Burst Pressures of Pipes Containing Dents and Gouges," Proc. Inst. Mech. Eng. Part E: J. Process Eng., **210**, pp. 19–27.

[4] Leis, B. N., Francini, R. B., Mohan, R., Rudland, D. L., and Olson, R. J., 1998, "Pressure-Displacement Behaviour of Transmission Pipelines Under Outside Forces Towards a Serviceability Criterion for Mechanical Damage," *Proceedings of the Eighth International Offshore and Polar Engineering Conference—ISOPE*, Montreal, Canada, J. S. Chung, M. Hisaaki, N. Shigeru, and I. Yoshiho, eds., Vol. 1, pp. 60–67.

[5] Kiefner, J. F., Maxey, W. A., Eiber, R. J., and Duffy, A. R., 1973, "Failure Stress Levels of Flaws in Pressurised Cylinders," Progress in Flaw Growth and Fracture Toughness Testing, American Society for Testing and Materials, ASTM STP 536, pp. 461–481.

[6] Alexander, C. R., 1999, "Review of Experimental and Analytical Investigations of Dented Pipelines," *Operations Applications, and Components*, I. T. Kisisel, I. Ezekoye, R. K. Lewis, B. M. Lory, O. B. Shirani, and J. Sinnappan, ASME, New York, Vol. 39, pp. 197–209.

[7] Cosham, A., Hopkins, P., 2003, "The Effect of Dents in Pipelines—Guidance in the Pipeline Defect Assessment Manual," *Proceedings of the Tenth International Conference on Pressure Vessel Technology*, ICPVT10, J. L. Zeman, ed., Oesterreichische Gesellschaft fuer Schweisstechnik, Vienna, pp. 111–119.

[8] Park, T. D., and Kyriakides, S., 1996, "On the Collapse of Dented Cylinders Under External Pressure," Int. J. Mech. Sci., **38**, pp. 557–578.

[9] Iflefel, I. B., 2006, "The Influence of Dents and Gouges on the Load Carrying Capacity of Transmission Pipelines," Ph.D. thesis, The University of Liverpool.

[10] Lancaster, E. R., 1993, "Behaviour of Pressurised Pipes Containing Dents and Gouges," Ph.D. thesis, Cambridge University.

[11] Ong, L. S., Soh, A. K., and Ong, J. H., 1992, "Experimental and Finite Element Investigation of a Local Dent on a Pressurised Pipe," J. Strain Anal. Eng. Des., **27**, pp. 177–185.

[12] Iflefel, I. B., Moffat, D. G., and Mistry, J., 2005, "The Interaction of Pressure and Bending on a Dented Pipe," Int. J. Pressure Vessels Piping, **82**, pp. 761–769.

[13] MSC/Patran, 2001, ra2, PDA Engineering Software Product Division, Santa Ana, CA.

[14] Hibbitt, Karlsson and Sorenson Inc., 2004, "ABAQUS Standard Users Manual," Version 6.4, Providence, Rhode Island, Pawtucket, RI.

[15] Ando, K., Takahashi, K., Hisatsune, M., and Hasegawa, K., "Failure Behaviour of Carbon Steel Pipe Having Local Wall Thinning Hear Tee Joint," *Proceedings of PVP2006-ICPVT-11 Conference*, Vancouver, Jul., ASME, Paper No. 93472, pp. 1–5.

Downloaded from http://asmedigitalcollection.asme.org/pressurevesseltech/article-pdf/130/2/021203/5534545/021203_1.pdf by guest on 05 November 2024